

Ultra compact and high resolution spectrometer based on optical transmission through submicron interferometer array

YANG T^{1,2}, LI C C², HO H P²

- (1. *Jiangsu Key Laboratory for Organic Electronics & Information Displays, Nanjing University of Posts and Telecommunications, Nanjing (210000), China;*
2. *Department of Electronic Engineering, Centre for Advanced Research in Photonics, The Chinese University of Hong Kong, Shatin, N. T., Hong Kong SAR, China)*

Abstract: We present an ultra compact and high resolution free space optical spectrometer and demonstrate it by using FDTD simulations. The miniature interferometer-based spectrometer is a series of submicron phase objects on a polymethyl methacrylate (PMMA) film with a CCD as the detector. The spectrum is obtained by solving a system of simultaneous linear equations. The Tikhonov regularization method is used to achieve a resolution at the picometer level. Compared with conventional spectrometers, the proposed device is low-cost and easy to fabricate due to its simple structure. Furthermore, its compact feature renders the device ideal for miniaturization and integration as the systems in microfluidics architectures and lab-on-chip designs.

Key words: Index terms; optical spectrometer; optical interferometer; Tikhonov regularization

1 Introduction

Absorption spectroscopy is an established method for the detection and analysis of chemical and biological samples extensively used in a wide range of industrial and research oriented applications^[1-3]. Fourier transform spectroscopy is one of the numerous spectroscopy techniques, distinguished by its unprecedented spectral discrimination paired with the inherent sensitivity^[4]. However current Fourier transform spectrometers, particularly those using scanning mirror mechanisms, do not fulfill the requirements of a small and easy-to-use sensor. Because such a compact and real-time operating analyzer could be used

for monitoring the quality of *e. g.* gasoline at gas stations, the quality and consistency of products (*e. g.* food and drug industry), the safety in fermentation environment (CO₂), and many other out-of-the lab applications. Grating based spectrometers have potentially more commercial market applications due to their small size^[5], but it also suffers disadvantages of low spectral resolution and expensive price.

In order to overcome the limitations of traditional devices and explore a more economical, compact and high performance spectrometer, we propose a novel interferometer-based spectrometer. The design process of the new device requires only the solution of a linear system. The miniature spectrometer has the combined advantages of low cost, small size and

high resolution. Its polymer structure can be built on a chip using existing fabrication technologies such as molding with the help of Focused Ion Beam (FIB) or Electron Beam Lithography (EBL), so the device is straightforward to fabricate.

2 Operating principle of spectrometer

As shown in Fig. 1, the design contains an interferometer array attached to a CCD chip. Each interferometer has two PMMA stages with a PMMA film as the substrate. The CCD pixel works as a detector beneath the PMMA substrate for each interferometer. Considering the Signal-to-Noise Ratio (SNR) and the sensitivity, we only use part of a CCD pixel as the detector for an interferometer by shading the remaining part.

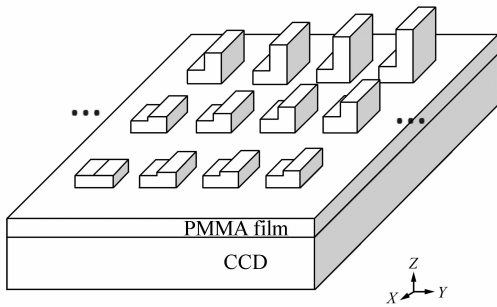


Fig. 1 Schematic of the optical spectrometer.

We enlarge the cross-section of the interferometer in Fig. 2 to demonstrate the principles of the device. When a plane wave illuminates the surfaces of the interferometer, the incoming beam is divided into two parts by the two stages of the interferometer. Because the height of each stage is different, the phase of each beam portion is separately delayed. When the two beam portions with different phase changes merge again, interference occurs and the interference intensity is measured by a CCD pixel underneath.

The detected intensity contains the spectral information. Since each frequency component in the

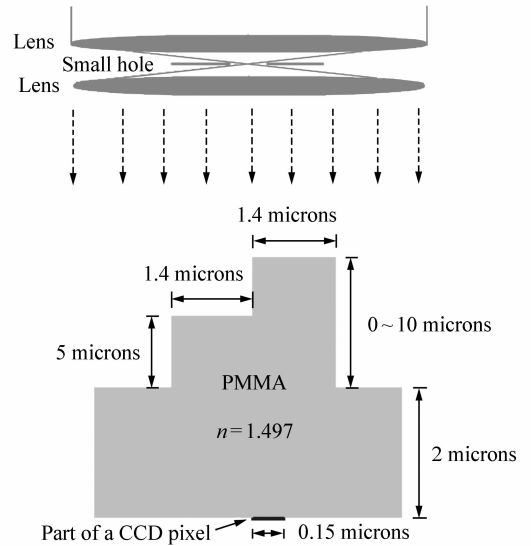


Fig. 2 Cross-section of the optical interferometer.

incoming beam corresponds to a unique phase difference of the two beam portions, the total intensity received by each CCD pixel, which results from the superposition of the interference signals from all the frequency components in the beam, should also be unique.

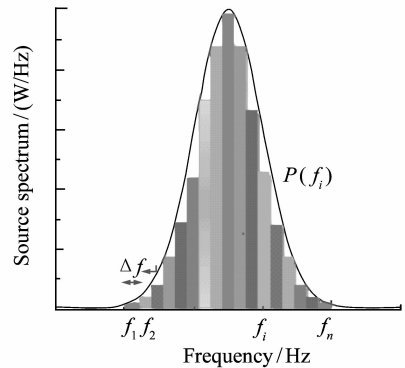


Fig. 3 Source spectrum used in simulation.

If the incoming beam is uniformly divided into n frequency components f_1, f_2, \dots, f_n with width Δf as shown in Fig. 3, the total power of the incoming beam can be calculated approximately by using integral calculus assuming n is large enough, *i. e.*

$$P_0 = P(f_1) \Delta f + P(f_2) \Delta f + \dots + P(f_n) \Delta f, \quad (1)$$

where $P(f_x)$ is the spectrum amplitude of f_x . After

passing through the interferometer, the measured power can be represented by

$$P = C_1 P(f_1) \Delta f + C_2 P(f_2) \Delta f + \dots + C_n P(f_n) \Delta f, \quad (2)$$

where C_1, C_2, \dots, C_n are transmission coefficients for the frequency parts f_1, f_2, \dots, f_n , respectively.

If the incoming beam illuminates n interferometers, a series of powers can be measured by the CCD array as follows

$$\begin{aligned} P_1 &= C_{11} P(f_1) \Delta f + C_{12} P(f_2) \Delta f + \dots \\ &\quad + C_{1n} P(f_n) \Delta f \\ P_2 &= C_{21} P(f_1) \Delta f + C_{22} P(f_2) \Delta f + \dots \\ &\quad + C_{2n} P(f_n) \Delta f \\ &\quad \dots\dots \\ P_n &= C_{n1} P(f_1) \Delta f + C_{n2} P(f_2) \Delta f + \dots \\ &\quad + C_{nn} P(f_n) \Delta f \end{aligned} \quad (3)$$

Therefore, given the transmission coefficients and the powers from different CCD pixels, *i. e.*

$$\mathbf{C} = \begin{pmatrix} C_{11} & C_{12} & \dots & C_{1n} \\ C_{21} & C_{22} & \dots & C_{2n} \\ \vdots & \vdots & \ddots & \vdots \\ C_{n1} & C_{n2} & \dots & C_{nn} \end{pmatrix} \quad (4)$$

$$\mathbf{A} = \begin{pmatrix} P_1 \\ P_2 \\ \vdots \\ P_n \end{pmatrix}, \quad (5)$$

we obtain a linear system

$$\mathbf{C}\mathbf{X} = \mathbf{A}, \quad (6)$$

where

$$\mathbf{X} = \begin{pmatrix} P(f_1) \cdot \Delta f \\ P(f_2) \cdot \Delta f \\ \vdots \\ P(f_n) \cdot \Delta f \end{pmatrix}. \quad (7)$$

Consequently, the spectrum of the incoming beam can be obtained by fitting $P(f_1), P(f_2), \dots, P(f_n)$, which are the elements of the matrix

$$\tilde{\mathbf{X}} = \mathbf{X} / \Delta f = \begin{pmatrix} P(f_1) \\ P(f_2) \\ \vdots \\ P(f_n) \end{pmatrix}. \quad (8)$$

Because the transmission coefficients can be determined by simulation or measurements, the spectrum reconstruction is the solution to Eq. (6). However, any data errors in the matrix \mathbf{A} due to the limited signal-to-noise ratio (SNR) make this linear system poorly defined. It is then difficult to solve such a large system of linear equations by using standard non-stationary iterative methods within the MATLAB environment. Here, we use the Tikhonov regularization method^[6] to solve Eq. (8).

The reconstruction normally takes about 1 s when $n = 2000$, so it enables real-time measurement for many applications. Although the fast Fourier transform (FFT) would require less time, its requirements are difficult to satisfy because beam portions coming from the two stages of an interferometer are not uniform in intensity due to the confinement and absorption of the waveguide. At the same time, partial interference of the two beam portions due to the structure layout also makes the FFT unfeasible.

3 Simulation results and discussion

We have performed a series of 2D simulation experiments by varying the height of one stage from 0 to 10 microns as demonstrated in Fig. 2. FDTD solutions (Lumerical Solutions, Inc) with a minimum 8 nm mesh size are used to study the interferometer structure. In order to smooth out edge effects^[7], we use a plane wave source that acts as a total-field scattered-field (TFSF) source with perfectly matched layer (PML) boundaries. The values in \mathbf{C} and \mathbf{A} can be obtained from a frequency domain power monitor by a series simulation experiments and the initial data can be analyzed by MATLAB.

Fig. 4 shows the final results on the comparisons between the reconstructed and original spectra with different values of α which is the data error of \mathbf{A} . In the figures, the solid lines are the original source spectrum; the dash lines are the reconstruction spectrum when α is equal to 1×10^{-8} ; and the dotted

lines are the reconstruction spectrum when α is equal to 3.5×10^{-7} . In Fig. 4(a) and Fig. 4(b), the dash lines almost coincide with the solid lines so that they are successful reconstructions. But the dotted line does not fully cover the solid line in Fig. 4(b), which means $\alpha = 3.5 \times 10^{-7}$ is not a suitable parameter for this ill-posed problem. In Fig. 4(c), neither the dotted line nor the dash line exactly covers the solid line. We can not reconstruct a perfect spectrum no matter how the value of α is chosen.

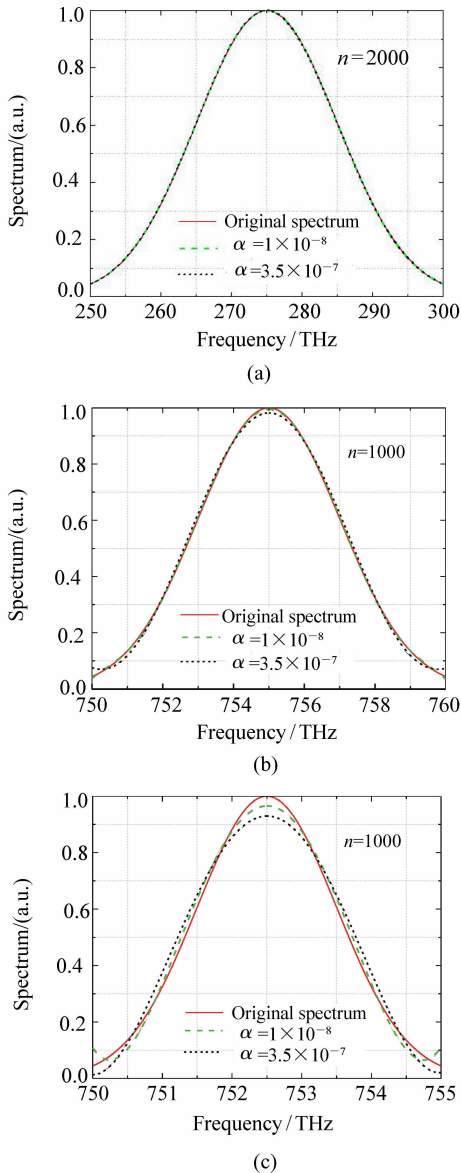


Fig. 4 Reconstruction with different values of α .

The simulation results also indicate that our de-

vice has the potential to achieve a very high resolution. Fig. 4(a) represents 2 000 frequency components that are reconstructed in the range from 250 THz to 300 THz, so the resolution is 25 GHz in frequency or 0.083 3 nm in wavelength; Fig. 4(b) represents 1 000 frequency components are reconstructed in the range from 750 THz to 760 THz, so the resolution is 10 GHz in frequency or 5.19 pm in wavelength; Fig. 4(c) represents 1 000 frequency components are reconstructed in the range from 750 THz to 755 THz. The frequency interval is even narrower, but distortion occurs. It is not a problem to solve for 2 000 or even more linear equations by using the Tikhonov regularization method. The limit of the resolution mainly depends on the sensitivity and the SNR of the CCD pixels in the experiments or the significant digits kept for values in simulation and calculation.

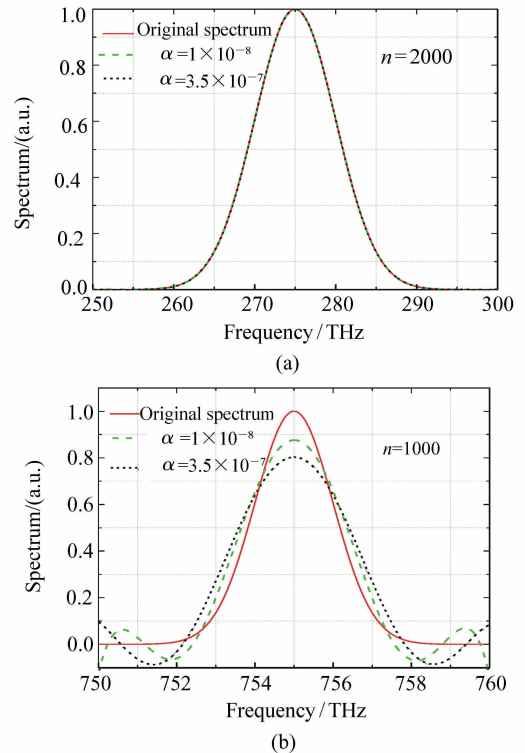


Fig. 5 Reconstruction of the original spectrum.

However, we also can investigate whether the shape of the original spectrum itself can affect the

good reconstructed spectrum which we can get. If there are a lot of zeroes in the original spectrum and the resolution is close to the limit, distortion may occur. The spectra in Fig. 4(a) and Fig. 5(a) have the same resolution and frequency range, so both of them represent successful reconstructions. However, the spectra in Fig. 4(b) and Fig. 5(b) also have the same resolution and frequency range while there are more zeroes in the original spectrum, as shown in Fig. 5(b), where an obvious distortion occurs because the resolution is close to the limit.

4 Other design considerations

One may also think about the crosstalk between the two interferometers. In the above simulation, the interferometers are studied individually assuming that they are optically isolated. The illumination width of the incoming beam is only $3.5\ \mu\text{m}$ in the above simulation that is sufficient enough to cover the major structure of the interferometer. However, Fig. 1 indicates that the interferometers should be assembled in an array configuration. In order to decrease the crosstalk between them, we need to separate the interferometers sufficiently. The distance between the two adjacent interferometers is $10\ \mu\text{m}$, so that a $1\ 000 \times 1\ 000$ array only occupies $1\ \text{cm}^2$. Therefore, the crosstalk problem can be solved by using a large enough spacing. In the following simulations, we set $\alpha = 1 \times 10^{-8}$ and keep the illumination width at $10\ \mu\text{m}$ for one interferometer as shown in Fig. 6. In order to explore the effects of Beam C and Beam D in Fig. 6, we reconstruct the same spectrum as shown in Fig. 4(a) and Fig. 4(b) with $10\ \mu\text{m}$ interval and show the results in Fig. 7. By comparing Fig. 7(a) with Fig. 4(a) and Fig. 7(b) with Fig. 4(b), we find all the corresponding simulations are almost identical. The original and reconstructed plots almost overlap with each other, so it can be concluded that the side illumination has little influence on the accuracy of reconstructions.

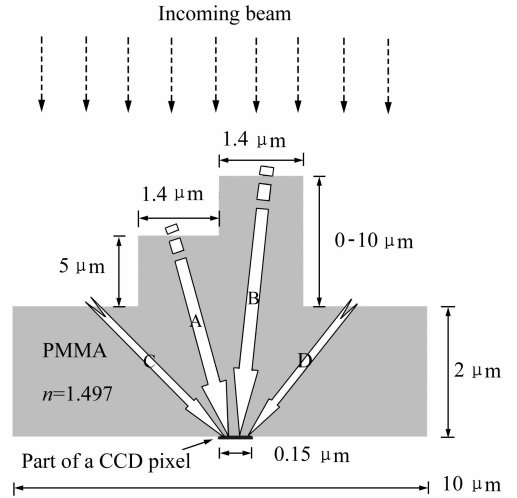


Fig. 6 Optical interference effect with side illumination.

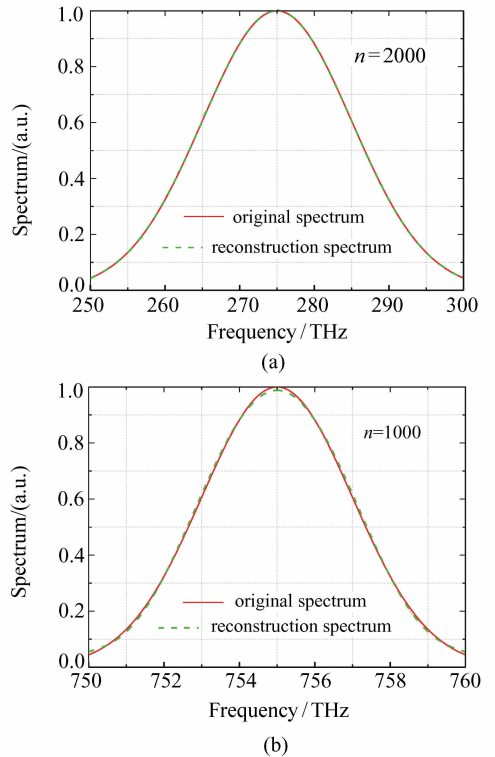


Fig. 7 Reconstruction with a large space interval ($10\ \mu\text{m}$).

We also explore other structures for the interferometer. Considering the difficulty in the fabricating of the extruded arrays, it would be simpler to adopt inverted pit structures. Both the extruded and the

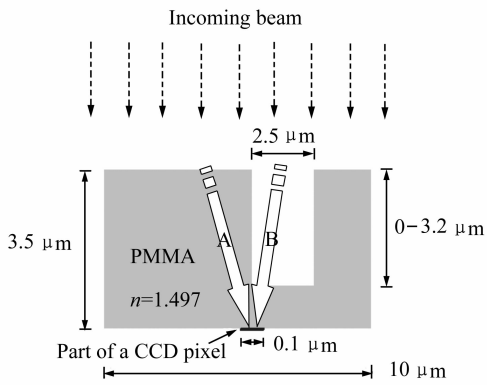
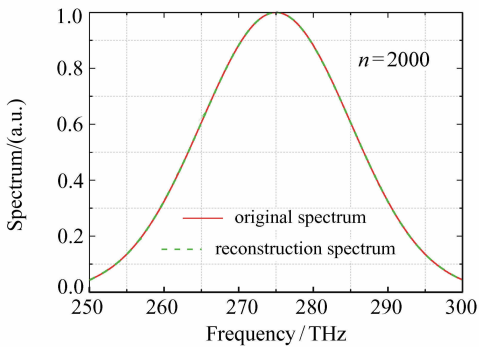
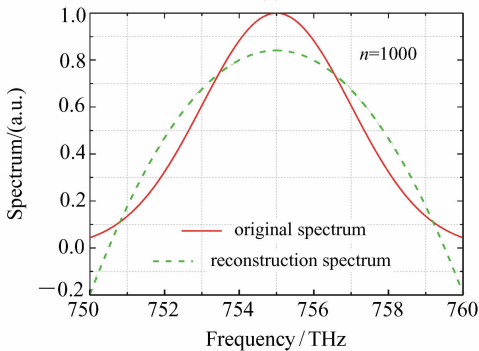


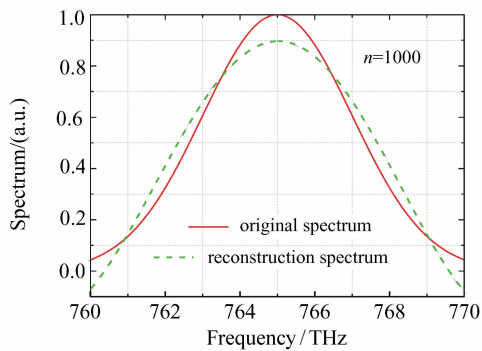
Fig. 8 Pit structure of interferometer.



(a)



(b)



(c)

Fig. 9 Reconstruction for pit structure.

pits can generate the required phase delay, so they can be used to realize the same function. The main advantage of the pit structure is that it is much easy to fabricate with current optical storage technology, *i. e.* we can fabricate the pit array with a model similar to the fabrication of CDs and DVDs. In order to further simplify the structure, we can just use one pit for an interferometer as shown in Fig. 8, because a single pit is sufficient to achieve the phase difference. Fig. 9 shows the reconstructed results of the simulation. However, in contrast to Fig. 9 (a), there is a large distortion in Fig. 9 (b) and Fig. 9(c). This means the resolution of the pit structure is inferior to that of the extruded structure. One explanation is that the positions of the monitors in the pit structure are further away from the polymer surface, so the detectors are more susceptible to distortion due to side illumination. Furthermore, the pits in the structure do not behave as waveguides, unlike the extruded structure.

5 Conclusions

We have proposed an ultra-compact and high-resolution free space optical spectrometer and quantified its operation using FDTD simulations. The Tikhonov regularization method is used to determine the resolution down to the picometer level. For a relatively simple structure, the proposed device is low-cost and easy to fabricate.

6 Acknowledgements

The authors would like to extend their appreciation to Mr. Zewen Wang of the East China Institute of Technology for his fruitful discussions and help with the Tikhonov regularization method and also to gratefully acknowledge the research studentship support for T. Yang from Chinese University of Hong Kong.

References :

- [1] ATAMAN C, UREY H. Compact Fourier transform spectrometers using FR4 platform[J]. *Sens. Actuators A*, 2009, 151: 9-16.
- [2] SCHLIESSER A, BREHM M, KEILMANN F. Frequency-comb infrared spectrometer for rapid, remote chemical sensing [J]. *Opt. Express*, 2005, 13: 9029-9039.
- [3] GEHM M E, JOHN R, BRADY D J, *et al.* . Single-shot compressive spectral imaging with a dual-disperser architecture [J]. *Opt. Express*, 2007, 15: 14013-14027.
- [4] ATAMAN C, UREY H, WOLTER A. A Fourier transform spectrometer using resonant vertical comb actuators [J]. *J. Micromech. Microeng.* , 2006, 16: 2517-2523.
- [5] YANG J Y, JUNG H, LEE G J, *et al.* . Micro-Electro-Mechanical-Systems-based infrared spectrometer composed of multi-slit grating and bolometer array [J]. *Jap. J. Appl. Phys.* , 2008, 47: 6943-6948.
- [6] HONERKAMP J, WEESE J. Tikhonov regularization method for ill-posed problems [J]. *Continuum Mech. Thermodyn.* , 1990, 2: 17-30.
- [7] Plane wave-Edge effects [EB/OL]. [2009-10-01]. http://www.lumerical.com/fdtd_online_help/user_guide_planewave_edge.php.

Author biographies: T. YANG was born in Zhenjiang, China, in 1978. He received his BSci and MEng in Department of Physics in Nanjing Normal University in 2001 and 2004 respectively. He took up a lecturing position in Nanjing University of Posts and Telecommunications from 2004. His PhD study is in the Chinese University of Hong Kong from 2006. He became a student member of IEEE in 2008. His research interests include optical spectrometers, photonic biosensors based on the surface plasmon resonance effect, optical memory, terahertz wave research and so on. He has over 20 journal/conference articles and 8 invention patents.

H. P. Ho received his BEng and PhD in Electrical and Electronic Engineering from the University of Nottingham in 1986 and 1990 respectively. His project title was on interdiffusion of semiconductor superlattices. During 1990 – 1992, he was a post-doctoral research fellow in the University of Leeds working on the growth and characterization of ferromagnetic superlattices. He then returned to University of Nottingham to participate in an industrial research project on laser ultrasound evaluation of engineering ceramics using high sensitivity laser interferometers. In 1994, he joined the Fiber Optics Components Operation of Hewlett-Packard as a senior process engineer in the semiconductor laser device fabrication division. He returned to Hong Kong to take up a lecturing position in the Department of Physics and Materials Science, City University of Hong Kong in 1996. He joined the Chinese University of Hong Kong in 2002. His research interests are currently optical instrumentation, particular biosensors based on the surface plasmon resonance effect, biophotonics and materials for optical applications. He has published over 150 journal/conference/book chapter articles. E-mail: hpho@ee.cuhk.edu.hk